



Research article

Salidroside ameliorates severe acute pancreatitis-induced cell injury and pyroptosis by inactivating Akt/NF- κ B and caspase-3/GSDME pathways

Xiaohong Wang^{a,*}, Jing Qian^b, Yun Meng^a, Ping Wang^a, Ruizhi Cheng^a, Guoxiong Zhou^c, Shunxing Zhu^d, Chun Liu^d

^a Department of Gastroenterology, Yizheng Hospital of Nanjing Drum Tower Hospital Group, Yizheng, 211900, Jiangsu, China

^b Department of General Surgery, Yizheng Hospital of Nanjing Drum Tower Hospital Group, Yizheng, 211900, Jiangsu, China

^c Department of Gastroenterology, Affiliated Hospital of Nantong University, Nantong, 226001, Jiangsu, China

^d Laboratory Animal Center of Nantong University, Nantong, 226001, Jiangsu, China



ARTICLE INFO

Keywords:

Salidroside
Severe acute pancreatitis
Pyroptosis
Inflammation
Akt/NF- κ B
Caspase-3/GSDME

ABSTRACT

Our previous studies showed that Salidroside (Sal), a glucoside of the phenylpropanoid tyrosol isolated from *Rhodiola rosea* L, alleviated severe acute pancreatitis (SAP) by inhibiting inflammation. However, the detailed mechanism remains unclear. Recent evidence has indicated a critical role of Sal in ameliorating inflammatory disorders by regulating pyroptosis. The present study aimed to explore the involvement of Sal and pyroptosis in the pathogenesis of SAP and investigate the potential mechanism. The effects of Sal on pyroptosis were first evaluated using SAP rat and cell model. Our results revealed that Sal treatment significantly decreased SAP-induced pancreatic cell damage and pyroptosis in vivo and in vitro, as well as reduced the release of lactate dehydrogenase (LDH), IL-1 β and IL-18. Search Tool for Interacting Chemicals (STITCH) online tool identified 4 genes (CASP3, AKT1, HIF1A and IL10) as candidate targets of Sal in both *rattus norvegicus* and *homo sapiens*. Western blot and immunohistochemistry staining validated that Sal treatment decreased the phosphorylation levels of Akt and NF- κ B p65, as well as cleaved caspase-3 and N-terminal fragments of GSDME (GSDME-N), suggesting that Sal might suppress pyroptosis through inactivating Akt/NF- κ B and Caspase-3/GSDME pathways. Furthermore, overexpression of AKT1 or CASP3 could partially reverse the inhibitory effects of Sal on cell injury and pyroptosis, while downregulation of AKT1 or CASP3 promoted the inhibitory effects of Sal. Taken together, our data indicate that Sal suppresses SAP-induced pyroptosis through inactivating Akt/NF- κ B and Caspase-3/GSDME pathways.

1. Introduction

Severe acute pancreatitis (SAP) represents 20% of the total cases of acute pancreatitis, one of the most diagnosed gastrointestinal disorders [1–3]. The disease is often associated with multiple organ failure, systemic inflammatory response syndrome, and a high mortality rate [4–6]. The mortality accounts for approximately 30% of all SAP cases [7]. To date, however, there is still no therapeutic agent available to block the disease course [3]. Thus, it is urgent to identify potential agents and explore the mechanism underlying

* Corresponding author.

E-mail address: wx102474wx@163.com (X. Wang).

<https://doi.org/10.1016/j.heliyon.2023.e13225>

Received 10 July 2022; Received in revised form 12 January 2023; Accepted 20 January 2023

Available online 28 January 2023

2405-8440/© 2023 The Authors. Published by Elsevier Ltd. This is an open access article under the CC BY-NC-ND license (<http://creativecommons.org/licenses/by-nc-nd/4.0/>).

SAP pathogenesis.

The pancreatitis is featured with pancreatic acinar cell injury and inflammatory cell infiltration [8,9]. When SAP occurs, macrophages infiltrate into the necrotic tissue, causing a systemic inflammatory response [10]. Growing evidence has shown that pancreatic acinar cells can form inflammasomes and die via pyroptosis, which contributes to SAP progression [11–13]. Pyroptosis is a novel pro-inflammatory type of programmed cell death initiated by inflammasomes, accompanied by caspase-mediated cleavage of gasdermins and release of inflammatory factors [14]. Pyroptosis has been implicated in many inflammatory diseases, such as systemic lupus erythematosus, Alzheimer's disease, sepsis and stroke [15–18]. But the detailed role of pyroptosis in SAP development has not been fully elucidated.

Salidroside (Sal, 2-(4-hydroxyphenethyl) ethyl- β -Dglucopyranoside) is one of the main bioactive compounds isolated from *Rhodiola rosea* L [19]. In recent years, Sal has been proven to play critical roles in regulating inflammation and pyroptosis [20]. For example, Sal could ameliorate Parkinson's and Alzheimer's disease through suppressing NLRP3-dependent pyroptosis [21,22]. In atherosclerosis, Sal significantly decreased atherosclerotic plaque and inhibited NLRP3-related endothelial cell pyroptosis [23]. Our previous studies demonstrated that Sal could obviously improve SAP-induced pancreatic damage partly through reducing inflammation [24,25]. These findings suggest that Sal might have a potential role to protect against SAP via inhibiting pancreatic acinar cell pyroptosis.

In this study, we aimed to explore the involvement of Sal and cell pyroptosis during SAP in vivo and in vitro. In addition, the molecular mechanism related to the process was also investigated, which might provide references for clinical treatment of SAP.

2. Materials and methods

2.1. Experimental design in vivo

The ethics and protocol were approved by the Yizheng Hospital of Nanjing Drum Tower Hospital Group Institutional Review Board. The 18 male Sprague-Dawley rats were randomly divided into 3 groups (n = 6 per group) for animal experiments as follows: (1) Negative control (sham) group; (2) SAP group, rats were administered with 3.5% sodium taurocholate solution according to our established protocol [26–28]; (3) SAP + Sal group, rats were received 20 mg/kg Sal (National Institutes for Food and Drug Control, Approval No. 110818–202009, Beijing, China) intraperitoneally 3 h after successful modeling. Sal injection (2 mg/ml) was prepared by dissolving 20 mg Sal in 10 ml double distilled water. This in vivo dose of Sal was selected mainly referring to our previous research [25]. After 24 h induction of SAP, all animals were euthanized, and blood and tissue samples were collected.

2.2. Cell culture and treatment

The rat pancreatic exocrine cell line AR42J was purchased from the China Center for Type Culture Collection (Wuhan, China). Cells were grown in Ham's F12 medium (Invitrogen) containing 10% fetal bovine serum and cultured in a 37 °C and 5% CO₂ incubator. To generate the cell model of SAP, AR42J cells were treated with 200 μ M tauroolithocholic acid 3-sulfate (TLC-S, Sigma, USA) and cells in the control group were cultured under normal conditions as our previously described [24]. For Sal treatment, the cells were incubated with 666 μ M Sal for additional 24 h according to our previous report [24], and then the cells and culture supernatants were collected for further studies.

2.3. Plasmids and oligonucleotides transfection

CV061-CMV-MCS-3FLAG-SV40-Puro-myrAKT1 plasmid with cDNA for constitutively active myristoylated rat AKT1 (CV-myr-AKT1), CV061-CMV-MCS-3FLAG-SV40-Puro-CASP3 with cDNA for rat CASP3 (CV-CASP3) and negative control (CV-NC), small interfering RNA (siRNA) specific for rat AKT1 (si-AKT1) and rat CASP3 (si-CASP3) and negative control (si-NC) were purchased by Genechem (Shanghai, China). Lipofectamine 2000 (Invitrogen) was used for transfections with 50 nM oligonucleotides or 100 nM plasmids following the manufacturer's protocol.

2.4. Cell counting kit-8 (CCK-8) assay

Cell viability was detected by CCK-8 assay. Cells at 6×10^3 cells per well were seeded in 96-well plates and incubated overnight. After 24 h inoculation, 10 μ l of CCK-8 reagent (#C0038, Beyotime, Shanghai, China) was added and cultured at 37 °C for 4 h. The absorbance at 450 nm was determined using a microplate reader (Thermo Scientific).

2.5. Histopathologic examination

Pancreatic tissues were fixed with 4% paraformaldehyde, and paraffin sectioned into 4 μ m thick sections. Then the sections were baked at 60 °C for 2 h, deparaffinized with xylene and rehydrated with gradient ethanol. Next, the sections were stained with hematoxylin (0.5 g/L, Mayer's hematoxylin) for 10 min and eosin (5 g/L) (HE) for 5 min. After baking at 37 °C for 30 min, the sections were mounted with neutral balsam, and the histopathologic changes were observed under a light microscope. The pancreatic tissue injury from 5 randomly selected fields in each section was evaluated by double-blind method and scored based on Schmidt's severity score standard of pancreas as follows: edema (0–4 points), inflammation (0–4 points), glandular cell necrosis (0–4 points) and

hemorrhage (0–1 point) [29].

2.6. Biochemical inspection

The serum and culture supernatants were collected. The activity of amylase were determined by Hitachi 7600 automatic biochemical analyzer (Hitachi). The levels of lactate dehydrogenase (LDH, #A020-2-2), TNF- α (#H052-1), IL-1 β (#H002), IL-6 (#H007-1-1), IL-8 (#H008) and IL-18 (#H015) were measured by assay kits from Jiancheng (Nanjing, China) according to the manufacturer's protocols.

2.7. Identification of candidate targets of Sal

Search Tool for Interacting Chemicals (STITCH, <http://stitch.embl.de>) is an online tool that predicts the potential interactions between proteins and chemicals in different organisms [30]. To identify candidate targets of Sal, we used "Single Item by Name/-Identifier" module. "Item Name" was set as "salidroside", "Organism" was set as "Homo sapiens" or "Rattus norvegicus" and "minimum required interaction score" was set as "medium confidence (0.4)".

2.8. Determination of Sal in pancreatic tissues by high performance liquid chromatography (HPLC)

After 1 h treatment of Sal, pancreatic tissues were collected and homogenized. Samples (200 μ l) were diluted with 1 ml methanol-water (50:50, v/v) and mixed by vibrating for 5 min. After centrifuging at 10,000 rpm for 20 min, the supernatant was collected, then freeze-dried and evaporated in vacuum. The residue was ultrasonically dissolved with 200 μ l mobile phase. After centrifuging at 10,000 rpm for 20 min, 20 μ l supernatant was injected and analyzed by HPLC. The Sal standard curve was established by mixing homogenized pancreatic tissues of sham group with a series of Sal standard samples with different concentrations analyzed by HPLC. The conditions were listed as follows: Welchrom C₁₈ column (4.6 mm \times 250 mm, 5 μ m); The mobile phase was acetonitrile-water (13:87, v/v); Volume flow was 1 ml/min; The detection wavelength was 275 nm; The column temperature is 30 $^{\circ}$ C.

2.9. Western blot

Cells were lysed by radio immunoprecipitation assay lysis buffer and proteins (30 μ g) were separated on 10% sodium dodecyl sulfate polyacrylamide gel electrophoresis and then transferred onto polyvinylidene fluoride membranes (Millipore). After blocked with blocking buffer (Beyotime) at room temperature for 30 min, the membranes were incubated with primary antibodies against p-Akt (1:1000; #4060, cst), Akt1 (1:1000; #2938, cst), NF- κ B p65 (1:1000; #8242, cst), NF- κ B p-p65 (1:1000; #ab86299, Abcam), cleaved caspase-3 (1:1000; #9664, cst), caspase-3 (1:1000; #9662, cst), GSDME (1:1000; ab215191, Abcam) and GAPDH (1:1000; #ab181602, Abcam) at 4 $^{\circ}$ C overnight. After incubation, the membranes were washed and incubated with HRP-conjugated secondary antibodies at room temperature for 2 h and visualized using the ECL system (Beyotime). Protein levels were normalized to GAPDH.

2.10. Hoechst 33342/propidium iodide (PI) double staining

Morphological changes of dead cells were detected by Hoechst 33342/PI Double Stain Kit (#CA1120, Solarbio, Beijing, China). Briefly, cells were seeded in 24-well plates for 24 h and received different treatments as indicated. The cells were then stained with Hoechst 33342 (10 μ g/ml) and PI (1 mg/ml) at 4 $^{\circ}$ C for 30 min and washed with phosphate buffered saline. Subsequently, the stained cells were observed under a fluorescence microscope (Leica).

2.11. Terminal deoxynucleotidyl transferase-mediated dUTP nick end-labeling (TUNEL) staining

Dead cells in pancreatic tissues were determined by TUNEL assay with an In Situ Cell Death Detection Kit (Roche, #11684809910) in compliance with the instructions. Then, the nucleus of the cells was stained with DAPI (0.4 μ g/ml, #S7113, Sigma) at room temperature for 10 min. TUNEL positive (green) and DAPI positive (blue) staining results were observed under a microscope. TUNEL-positive cells from 5 randomly selected fields were counted.

2.12. Immunohistochemistry (IHC) staining analysis

The collected pancreatic tissues were fixed in 4% paraformaldehyde at 4 $^{\circ}$ C overnight, paraffin-embedded and sectioned into 5- μ m thick sections. Then the sections were dewaxed with gradient ethanol, steam heated for antigen retrieval in citrate-based buffer, blocked with 3% H₂O₂ followed by 10% bovine serum albumin. Then, the sections were incubated with anti-NF- κ B p-p65 primary antibody (1:200, #ab86299, abcam) overnight at 4 $^{\circ}$ C and secondary antibody (1:2000, Abcam) for 1 h at room temperature, and stained with a DAB and hematoxylin substrate kit (ZSGB-BIO, Beijing, China).

2.13. Immunofluorescence staining

Treated cells were fixed with 4% polyformaldehyde at room temperature for 20 min and then permeabilized with 0.5% Triton X-

100 for 10 min. After blocking with 5% goat serum for 30 min, the cells were incubated with primary antibody against p65 (1:2000, #8242, cst) at 4 °C overnight and then incubated with fluorescent secondary antibody. The nucleus was stained with DAPI (0.4 µg/ml, #S7113, Sigma). Slides were visualized under a fluorescence microscopy.

2.14. Statistical analysis

Data were expressed as the mean \pm standard deviation (SD) of at least three separate experiments. All data analysis was conducted using GraphPad Prism 9 (GraphPad Software, USA). The unpaired *t*-test and one-way analysis of variance (ANOVA) were performed for comparisons between two or multiple groups. Statistical significance was set at $P < 0.05$.

3. Results

3.1. Sal suppressed SAP-induced cell pyroptosis in vivo

To explore the involvement of Sal and pyroptosis during SAP, we established SAP rat model and then treated with Sal. HPLC analysis showed that the retention time of Sal was 6.5 min (Supplementary Fig. 1). After 1 h treatment of Sal, the concentration of Sal in pancreatic tissues was 0.37 ± 0.02 µg/ml. HE staining demonstrated that there was no abnormal change in pancreatic acini and stroma in the sham group, and the other groups showed different degrees of SAP pathological changes, such as edema, hemorrhage, necrosis, inflammatory cell infiltration and incomplete lobules (Fig. 1A and B). In the SAP group, large areas of necrosis, extensive congestion and edema, many infiltrated inflammatory cells and red blood cells in the stroma and acini were observed, along with microthrombosis. Meanwhile, the structure of lobules and acini were fuzzy or even complete destroyed in the SAP group. In the SAP + Sal group, the lesion degree in the necrosis, hemorrhage, edema and inflammation of pancreatic tissue was reduced compared with the SAP group. As shown in Fig. 1C and D, the number of TUNEL-positive cells was obviously increased following SAP treatment, but the

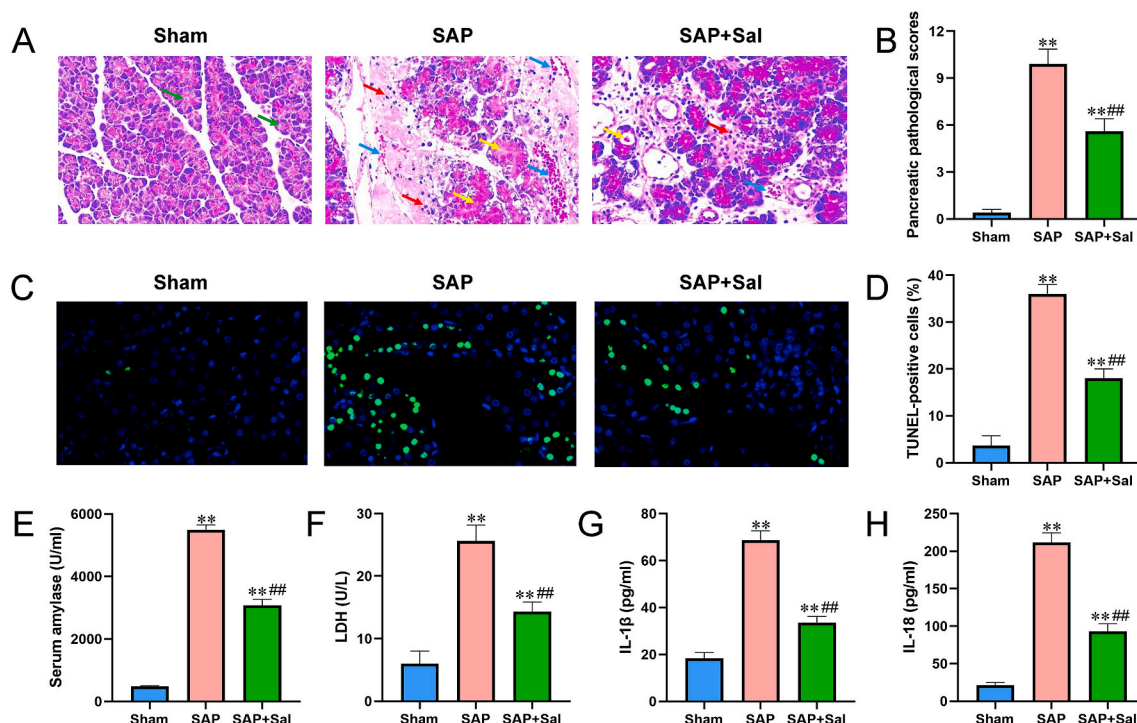


Fig. 1. Sal suppressed SAP-induced cell pyroptosis in vivo. **A** Representative images of HE stained sections of rat pancreatic tissues from sham, SAP and SAP + Sal group. \rightarrow represented lobule structure, \rightarrow represented microthrombosis, \rightarrow represented red cells and \rightarrow represented immune cells. **B** Quantitative analysis of pancreatic injury score. The histopathologic changes of Fig. 1A were observed under a light microscope. Five non-overlapping visual fields were randomly selected in each section and the pancreatic tissue injury was evaluated by double-blind method and scored based on Schmidt's severity score standard of pancreas as follows: edema (0–4 points), inflammation (0–4 points), glandular cell necrosis (0–4 points) and hemorrhage (0–1 point). **C** Representative images of TUNEL staining of rat pancreatic tissues from sham, SAP and SAP + Sal group. Blue represents DAPI staining and green represents TUNEL staining. **D** Quantitative analysis of TUNEL-positive cells. TUNEL-positive cells from 5 randomly selected fields were observed and counted under a microscope. The data were expressed as mean \pm standard deviation. **E** Activity of the serum amylase. **F** LDH release in the pancreatic tissues. **G** Serum IL-1 β level. **H** Serum IL-18 level. ** $P < 0.01$ compared with sham group. ### $P < 0.01$ compared with SAP group. (For interpretation of the references to colour in this figure legend, the reader is referred to the Web version of this article.)

percentage of TUNEL-positive cells was reduced by approximately 50% with Sal treatment. Besides, activity of the serum amylase was significantly lower in SAP + Sal group than that of SAP group (Fig. 1E). Compared with sham group, the LDH release, IL-1 β and IL-18 levels were prominently increased in SAP group, but the levels were evidently decreased with Sal treatment (Fig. 1F-H).

3.2. Sal suppressed SAP-induced cell injury and pyroptosis in AR42J cells

To further evaluate the functions of Sal in pyroptosis, AR42J cells were incubated with TLC-S. As observed by microscopy, cells treated with SAP notably exhibited morphological features of pyroptotic cells, with swelling and balloon-like bubbling, while the number of pyroptotic cells was reduced after Sal treatment (Fig. 2A). CCK-8 assay results showed that cell viability was inhibited with TLC-S treatment, but enhanced after Sal treatment compared with SAP alone (Fig. 2B). Hoechst 33342/PI double staining validated that SAP-induced pyroptosis was partly mitigated by Sal treatment in AR42J cells (Fig. 2C and D). Consistent with *in vivo* experiments, the activity of amylase was increased in SAP group in comparison with control group (Fig. 2E). However, the activity of amylase was reduced with Sal treatment. Furthermore, Sal treatment also suppressed the LDH release, IL-1 β and IL-18 production levels (Fig. 2F-H). These findings indicate that Sal could relieve SAP-induced cell injury and pyroptosis.

3.3. Sal suppressed activation of Akt/NF- κ B and caspase-3/GSDME pathways

To uncover the underlying mechanism through which Sal regulated cell pyroptosis in SAP, an online tool STITCH was used to predict the possible targets of Sal. As shown in Fig. 3A and B, 4 genes (CASP3, AKT1, HIF1A and IL10) were identified as candidate targets of Sal in both *rattus norvegicus* and *homo sapiens*. Recent studies have indicated that Akt/NF- κ B and Caspase-3/GSDME pathways play a key role in regulating cell pyroptosis [31–34]. Western blot analysis was performed to measure the protein levels of Akt/NF- κ B and Caspase-3/GSDME pathways-related genes. The results revealed that Sal treatment reduced the levels of p-Akt, p-p65, cleaved caspase-3 and N-terminal fragments of GSDME (GSDME-N) (Fig. 3C and D and Supplementary Fig. 2). Immunofluorescence analysis showed that SAP treatment caused a translocation of p65 into the nucleus, but Sal reversed this translocation (Fig. 3E). In addition, we detected the expression of NF- κ B p-p65 in the pancreatic tissues by IHC staining. The data showed that Sal

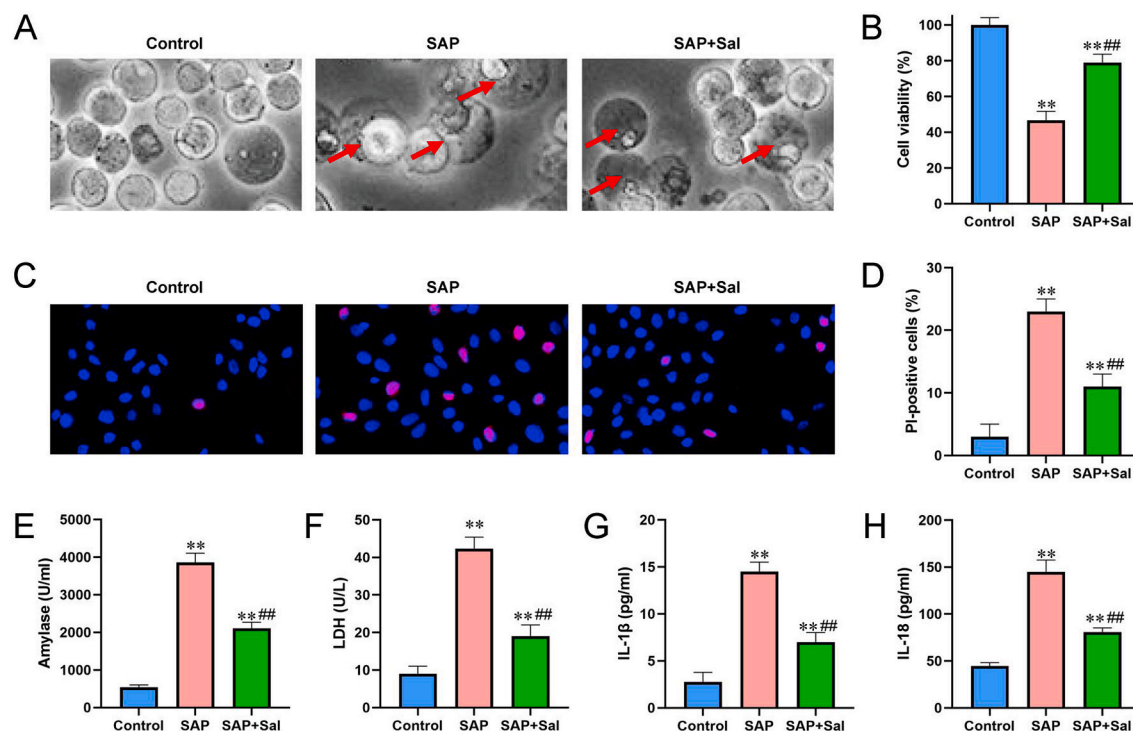


Fig. 2. Sal suppressed SAP-induced cell injury and pyroptosis in AR42J cells. **A** Representative morphological images of AR42J cells treated with SAP or SAP + Sal under microscope. \rightarrow represented pyroptotic cells. **B** AR42J cells were treated with SAP or SAP + Sal and then cell viability was determined by CCK-8 assay with an absorbance at 450 nm. **C** Representative images of Hoechst 33342/PI double staining. Blue represents Hoechst 33342 staining and red represents PI staining. **D** Quantitative analysis of PI-positive cells. PI-positive cells from 5 randomly selected fields were observed and counted under a fluorescence microscope. The data were expressed as mean \pm standard deviation. **E** Amylase activity in the cultured cell supernatant. **F** LDH release in the cultured cell supernatant. **G** IL-1 β level in the cultured cell supernatant. **H** IL-18 level in the cultured cell supernatant. ** $P < 0.01$ compared with control group. ## $P < 0.01$ compared with SAP group. (For interpretation of the references to colour in this figure legend, the reader is referred to the Web version of this article.)

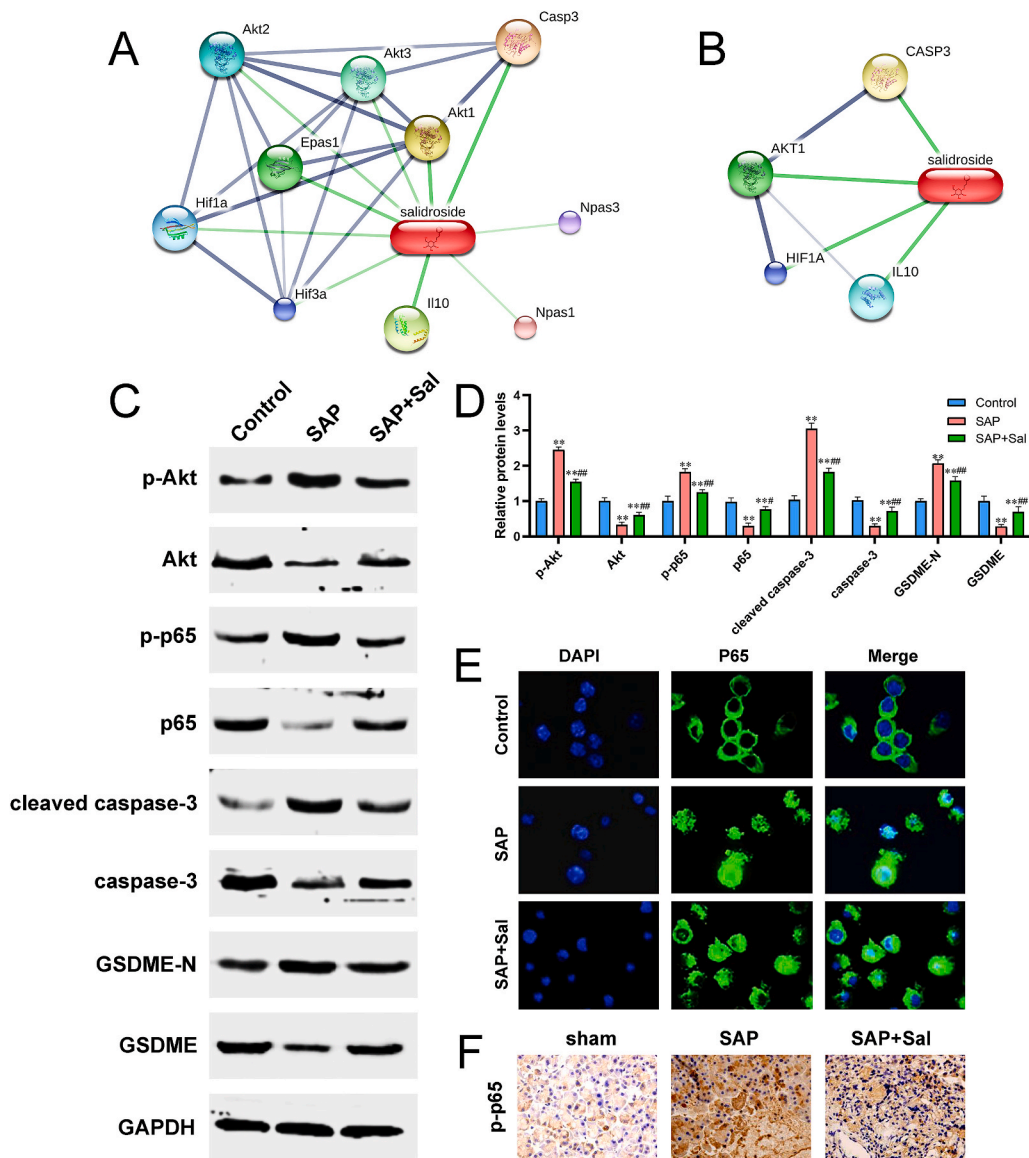


Fig. 3. Sal suppressed activation of Akt/NF-κB and Caspase-3/GSDME pathways. **A** Ten proteins (Akt1, Akt2, Akt3, Casp3, Epas1, Hif1α, Hif3α, IL10, Npas1 and Npas3) were predicted to be potential targets of Sal in *rattus norvegicus* by an online tool STITCH. **B** Four proteins (AKT1, CASP3, HIF1A and IL10) were predicted to be potential targets of Sal in *homo sapiens* by STITCH. **C** Effects of Sal on Akt/NF-κB and Caspase-3/GSDME pathways-related proteins were evaluated by Western blot in SAP cell model. **D** Quantitative analysis of relative protein levels of Fig. 3C. **E** Effect of Sal on the nuclear translocation of p65 was determined by immunofluorescence. **F** IHC staining of p-p65 in the rat pancreatic tissues. **P < 0.01 compared with control group. #P < 0.05, ##P < 0.01 compared with SAP group.

treatment could reduce the expression level of p-p65 compared with SAP group (Fig. 3F). Taken together, these results demonstrated that inactivation of Akt/NF-κB and Caspase-3/GSDME pathways might be responsible for Sal suppressing SAP-induced pyroptosis.

3.4. Sal ameliorated SAP-induced cell injury and inflammation by inhibiting AKT1 and CASP3 expression

To further validate the involvement of Akt/NF-κB and Caspase-3/GSDME pathways in the Sal-mediated protection against SAP, CV-myrAKT1, CV-CAPS3, si-AKT1 or si-CASP3 were transiently transfected into AR42J cells. As shown in Fig. 4A and B, the efficiency of overexpression and downregulation was verified by Western blot (Supplementary Fig. 3). CV-myrAKT1 or CV-CAPS3 reversed the promotion of cell viability-induced by Sal treatment, and si-AKT1 or si-CASP3 further increased cell viability in comparison to negative control group (Fig. 4C). Furthermore, Sal treatment decreased the activity of the amylase, nevertheless, overexpression of AKT1 or CAPS3 presented opposite results, and downregulation of AKT1 or CAPS3 significantly reduced the activity of the amylase compared with negative control group (Fig. 4D).

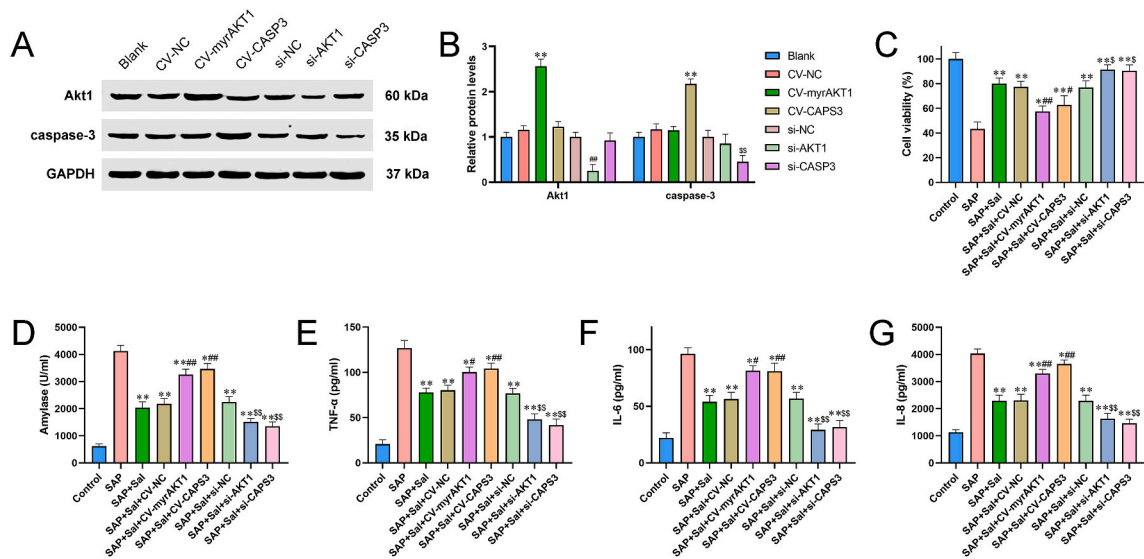


Fig. 4. Sal ameliorated SAP-induced cell injury and inflammation by inhibiting AKT1 and CASP3 expression. **A** AR42J cells were transfected with CV-myrAKT1, CV-CAPS3, si-AKT1, si-CASP3 or negative controls. The efficiency of overexpression and downregulation was verified by Western blot. **B** Quantitative analysis of relative protein levels of Fig. 4A. **C** Cell viability was detected by CCK-8 assay. **D-G** AR42J cells were transfected with CV-myrAKT1, CV-CAPS3, si-AKT1, si-CASP3 or negative controls and then treated with SAP and Sal. Amylase activity (**D**), TNF- α level (**E**), IL-6 level (**F**) and IL-8 level (**G**) in the cultured cell supernatant. For **B**, ** $P < 0.01$ compared with CV-NC group. For **C-G**, * $P < 0.05$, ** $P < 0.01$ compared with SAP group. # $P < 0.05$, ## $P < 0.01$ compared with SAP + Sal + CV-NC group. \$ $P < 0.05$, \$\$ $P < 0.01$ compared with SAP + Sal + si-NC group.

Our previous studies indicated that Sal could suppress the inflammation, meanwhile pyroptosis is an inflammatory form of programmed cell death. Thus, we supposed that Akt/NF- κ B and Caspase-3/GSDME pathways might participate in the Sal-mediated inflammatory response in SAP. ELISA assays results indicated that the overexpression of AKT1 or CAPS3 reversed, and downregulation of AKT1 or CAPS3 enhanced the inhibitory effect of Sal on pro-inflammatory cytokine production of TNF- α , IL-6 and IL-8 (Fig. 4E–4G). Taken together, our data indicate that Sal could alleviate SAP-induced cell injury and inflammation partly through Akt/NF- κ B and Caspase-3/GSDME pathways.

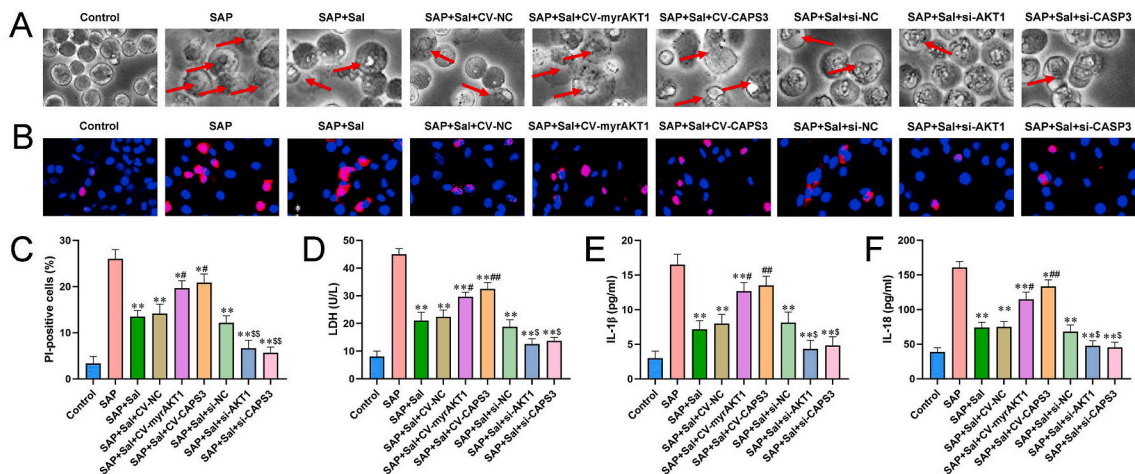


Fig. 5. Sal suppressed SAP-induced cell pyroptosis through reducing AKT1 and CASP3 expression. AR42J cells were transfected with CV-myrAKT1, CV-CAPS3, si-AKT1, si-CASP3 or negative controls and then treated with SAP and Sal. **A** Representative morphological images of AR42J cells under microscope. \rightarrow represented pyroptotic cells. **B** Representative images of Hoechst 33342/PI double staining. Blue represents Hoechst 33342 staining and red represents PI staining. **C** Quantitative analysis of PI-positive cells. **D-F** LDH release (**D**), IL-1 β level (**E**) and IL-18 level (**F**) in the cultured cell supernatant. * $P < 0.05$, ** $P < 0.01$ compared with SAP group. # $P < 0.05$, ## $P < 0.01$ compared with SAP + Sal + CV-NC group. \$ $P < 0.05$, \$\$ $P < 0.01$ compared with SAP + Sal + si-NC group. (For interpretation of the references to colour in this figure legend, the reader is referred to the Web version of this article.)

3.5. Sal suppressed SAP-induced cell pyroptosis through reducing AKT1 and CASP3 expression

Subsequently, we determined whether Sal inhibiting SAP-induced cell pyroptosis was dependent on Akt/NF- κ B and Caspase-3/GSDME pathways. We observed that Sal treatment could alleviate the SAP-induced cell pyroptosis, whereas AKT1 or CASP3 overexpression partially removed this alleviation, and AKT1 or CASP3 silence further reduced the number of pyroptotic cells compared with negative control group (Fig. 5A). Moreover, Hoechst 33342/PI double staining confirmed that Sal treatment remarkably decreased the number of PI-positive cells, whereas the number of PI-positive cells was increased when CV-myrAKT1 or CV-CASP3 was transfected into AR42J cells (Fig. 5B and C). Meanwhile, silence of AKT1 or CASP3 decreased the number of PI-positive cells. As shown in Fig. 5D, we noted that overexpression of AKT1 or CASP3 reversed the Sal-induced inhibition of LDH release, while downregulation of AKT1 or CASP3 further promoted the Sal-induced effects on LDH release. Similarly, the reduction of IL-1 β and IL-18 production levels was diminished following with the overexpression of AKT1 or CASP3, but the reduction tendency was obviously accelerated after silencing AKT1 or CASP3 (Fig. 5E and F). These results imply that Sal exerts its protective role against SAP-induced pyroptosis at least in part via regulating Akt/NF- κ B and Caspase-3/GSDME pathways.

4. Discussion

Pancreatic acinar cell death is an important event in the progression of SAP due to relevant inflammatory cascade. In recent years, various forms of cell death have been characterized during SAP, including apoptosis, necrosis, autophagy, ferroptosis and pyroptosis [35–38]. The form of pancreatic acinar cell death is closely related to the prognosis of SAP patients. As two main death forms of pancreatic acinar cells in SAP, the transformation from necrosis to apoptosis can reduce the severity and has a beneficial effect on the prognosis [39]. Different from apoptosis, however, pyroptosis triggers an excessive release of pro-inflammatory cytokines and eventually aggravates pancreatic injury [12]. In this context, understanding the molecular mechanism of pancreatic acinar cell pyroptosis might contribute to the SAP treatment.

Recently, many studies have focused on the role of pyroptosis in SAP pathogenesis. For example, downregulated Gasdermin D (GSDMD) was reported to reduce SAP-induced pyroptosis and relieve the pancreatic and intestinal mucosal damage in a mouse model [40]. Xu et al. found that emodin treatment significantly mitigated the SAP-associated pyroptosis, inflammation and lung damage through activating NLRP3/IL-1 β /CXCL1 signaling via downregulating CIRP expression [41]. Consistent with the findings mentioned above, we observed obvious morphological features of pyroptotic cells in SAP cell model. Sal treatment could significantly reduce the SAP-induced pyroptosis and inflammatory response. In recent studies, the involvement of Sal and pyroptosis has also been implicated in Parkinson's disease, Alzheimer's disease and atherosclerosis [21–23]. Taken together, these studies support an unequivocal role for Sal in inhibiting pyroptosis under pathological conditions.

Recently, we explored the underlying mechanisms by which Sal exerted its inhibitory effects on cell pyroptosis during SAP. Based on STITCH prediction and previous literature reports, we assumed that AKT1 and CASP3 might be crucial downstream targets of Sal. Western blot results demonstrated that Sal could decrease the levels of p-Akt and cleaved caspase-3, as well as their downstream p-p65 and GSDME-N expression. Furthermore, Sal treatment suppressed p65 translocation from cytoplasm to nucleus. More importantly, rescue experiments further confirmed that overexpression of AKT1 and CASP3 could reverse the inhibitory effects of Sal on cell injury and pyroptosis, while downregulation of AKT1 and CASP3 further promoted the effects of Sal. Thus, we concluded that Sal ameliorated SAP-induced pyroptosis at least partially by inactivating Akt/NF- κ B and Caspase-3/GSDME pathways.

Akt/NF- κ B pathway is an important cellular signaling cascade that widely involves in the inflammatory diseases [42–44]. Previous studies have indicated that Akt is a key downstream of Sal. For instance, Sal treatment was reported to protect against H₂O₂-induced endothelial dysfunction by activating AMPK, Akt and NF- κ B [45]. Whereas, a recent study from He et al. demonstrated that Sal pretreatment with hypoxia could increase the ability of rat adipose-derived stem cell proliferation, migration and tolerance against H₂O₂-induced oxidative stress by activating Akt and inactivating NF- κ B pathway [46]. Growing evidence has also suggested a regulatory function of Sal in regulating caspase-3 expression. Tang et al. discovered that Sal suppressed apoptosis of PC12 cells by reducing cleaved caspase-3 and caspase-3 expression [47]. Interestingly, other studies have reported conflicting results. In thyroid cancer WRO cells, Sal significantly restrained cell migration and invasion, and induced apoptosis by activating JAK2/STAT3 pathway and promoting cleaved caspase-3 level [48]. These findings suggest that Sal could regulate Akt/NF- κ B and Caspase-3/GSDME pathways, but the activation or inactivation might differ in different diseases. Moreover, further investigations will be needed to elucidate the mechanism by which Sal regulates the expression of Akt and caspase-3.

There were several limitations to this study. AKT1 and CASP3 were predicted to be potential targets of Sal, and our experimental data also showed Sal could regulate AKT1 and caspase-3 expression. However, these findings did not provide evidence for the direct interaction between Sal and AKT1 or caspase-3. Molecular docking and fluorescent-labeled probe of Sal will help to validate these findings. In addition, the effects of AKT1 and CASP3 on Sal-mediated pyroptosis and inflammation were tested by SAP cell model in vitro, which is worthy of further investigations using in vivo SAP model. Furthermore, although our studies indicate that Sal shows a potential protective effect against SAP by ameliorating pancreatic injury via regulating cell pyroptosis and inflammatory response, it is still a long way to go before Sal use in clinic. Like many clinical translations of natural molecules, we need to overcome lots of problems, such as bioavailability, safety and pharmacodynamic reproducibility [49].

In summary, this study indicated that Sal could suppress SAP-induced pancreatic injury, pyroptosis and inflammation in a Akt/NF- κ B and Caspase-3/GSDME pathways-dependent manner. Our findings also added novel insights into the mechanism of Sal against SAP and highlighted the potential of Sal as a therapeutic agent for SAP intervention.

Ethical approval

The study protocols of all animal experiments were approved by the Yizheng Hospital of Nanjing Drum Tower Hospital Group Institutional Review Board. All procedures were performed in accordance with the ARRIVE guidelines and the Guidelines for the Care and Use of Laboratory Animals.

Author contribution statement

Xiaohong Wang: Conceived and designed the experiments; Contributed reagents, materials, analysis tools or data; Performed the experiments; Analyzed and interpreted the data; Wrote the paper.

Yun Meng, Ping Wang, Ruizhi Cheng, Guoxiong Zhou, Shunxing Zhu and Chun Liu: Contributed reagents, materials, analysis tools or data; Performed the experiments; Analyzed and interpreted the data.

Jing Qian: Contributed reagents, materials, analysis tools or data; Performed the experiments; Analyzed and interpreted the data; Wrote the paper.

Funding statement

Dr. Xiaohong Wang was supported by the Traditional Chinese Medicine Technology Development Plan Project of Jiangsu Province in 2020 [YB2020088], the Key R&D Projects in Yangzhou City in 2021 (Social Development) [YZ2021091], and the Health Innovation Project of Lvyang Jinfeng Plan of Yangzhou City in 2020 [YZLYJF2020WSCX037].

Data availability statement

Data included in article/supp. material/referenced in article.

Declaration of interest's statement

The authors declare no conflict of interest.

Appendix A. Supplementary data

Supplementary data related to this article can be found at <https://doi.org/10.1016/j.heliyon.2023.e13225>.

References

- [1] M. Portelli, C.D. Jones, Severe acute pancreatitis: pathogenesis, diagnosis and surgical management, *Hepatobiliary Pancreat. Dis. Int.* 16 (2) (2017) 155–159.
- [2] G.I. Papachristou, Prediction of severe acute pancreatitis: current knowledge and novel insights, *World J. Gastroenterol.* 14 (41) (2008) 6273–6275.
- [3] A. Habtezion, A.S. Gukovskaya, S.J. Pandol, Acute pancreatitis: a multifaceted set of organelle and cellular interactions, *Gastroenterology* 156 (7) (2019) 1941–1950.
- [4] M.A. Mederos, H.A. Reber, M.D. Gargis, Acute pancreatitis: a review, *JAMA* 325 (4) (2021) 382–390.
- [5] V.K. Singh, B.U. Wu, T.L. Bollen, K. Repas, R. Maurer, K.J. Mortele, P.A. Banks, Early systemic inflammatory response syndrome is associated with severe acute pancreatitis, *Clin. Gastroenterol. Hepatol.* 7 (11) (2009) 1247–1251.
- [6] E. Zarem, Treatment of severe acute pancreatitis and its complications, *World J. Gastroenterol.* 20 (38) (2014) 13879–13892.
- [7] P.G. Lankisch, M. Apte, P.A. Banks, Acute pancreatitis, *Lancet* 386 (9988) (2015) 85–96.
- [8] M. Sandler, S. Maertin, D. John, M. Persike, F.U. Weiss, B. Krüger, T. Wartmann, P. Wagh, W. Halang, N. Schaschke, J. Mayerle, M.M. Lerch, Cathepsin B activity initiates apoptosis via digestive protease activation in pancreatic acinar cells and experimental pancreatitis, *J. Biol. Chem.* 291 (28) (2016) 14717–14731.
- [9] P.S. Leung, S.P. Ip, Pancreatic acinar cell: its role in acute pancreatitis, *Int. J. Biochem. Cell Biol.* 38 (7) (2006) 1024–1030.
- [10] M. Sandler, A. Dummer, F.U. Weiss, B. Krüger, T. Wartmann, K. Scharfetter-Kochanek, N. van Rooijen, S.R. Malla, A. Aghdassi, W. Halang, M.M. Lerch, J. Mayerle, Tumour necrosis factor α secretion induces protease activation and acinar cell necrosis in acute experimental pancreatitis in mice, *Gut* 62 (3) (2013) 430–439.
- [11] M. Sandler, C. van den Brandt, J. Glaubitz, A. Wilden, J. Golchert, F.U. Weiss, G. Homuth, L.L. De Freitas Chama, N. Mishra, U.M. Mahajan, L. Bossaller, U. Völker, B.M. Bröker, J. Mayerle, M.M. Lerch, NLRP3 inflammasome regulates development of systemic inflammatory response and compensatory anti-inflammatory response syndromes in mice with acute pancreatitis, *Gastroenterology* 158 (1) (2020) 253–269.e14.
- [12] L. Gao, X. Dong, W. Gong, W. Huang, J. Xue, Q. Zhu, N. Ma, W. Chen, X. Fu, X. Gao, Z. Lin, Y. Ding, J. Shi, Z. Tong, T. Liu, R. Mukherjee, R. Sutton, G. Lu, W. Li, Acinar cell NLRP3 inflammasome and gasdermin D (GSDMD) activation mediates pyroptosis and systemic inflammation in acute pancreatitis, *Br. J. Pharmacol.* 178 (17) (2021) 3533–3552.
- [13] J. Wang, X. Li, Y. Liu, C. Peng, H. Zhu, G. Tu, X. Yu, Z. Li, CircHIPK3 promotes pyroptosis in acinar cells through regulation of the miR-193a-5p/GSDMD Axis, *Front. Med.* 7 (2020) 88.
- [14] F. Humphries, L. Shmuel-Galia, N. Ketelut-Carneiro, S. Li, B. Wang, V.V. Nemmara, R. Wilson, Z. Jiang, F. Khalighinejad, K. Muneeruddin, S.A. Shaffer, R. Dutta, C. Ionete, S. Pesiridis, S. Yang, P.R. Thompson, K.A. Fitzgerald, Succination inactivates gasdermin D and blocks pyroptosis, *Science* 369 (6511) (2020) 1633–1637.
- [15] Y. Huang, D.D. Yang, X.Y. Li, D.L. Fang, W.J. Zhou, ZBP1 is a significant pyroptosis regulator for systemic lupus erythematosus, *Ann. Transl. Med.* 9 (24) (2021) 1773.
- [16] C. Han, Y. Yang, Q. Guan, X. Zhang, H. Shen, Y. Sheng, J. Wang, X. Zhou, W. Li, L. Guo, Q. Jiao, New mechanism of nerve injury in Alzheimer's disease: β -amyloid-induced neuronal pyroptosis, *J. Cell Mol. Med.* 24 (14) (2020) 8078–8090.

- [17] Y.L. Gao, J.H. Zhai, Y.F. Chai, Recent advances in the molecular mechanisms underlying pyroptosis in sepsis, *Mediat. Inflamm.* 2018 (2018), 5823823.
- [18] J. Wang, J. Yao, Y. Liu, L. Huang, Targeting the gasdermin D as a strategy for ischemic stroke therapy, *Biochem. Pharmacol.* 188 (2021), 114585.
- [19] Y. Mao, Y. Li, N. Yao, Simultaneous determination of salidroside and tyrosol in extracts of *Rhodiola L.* by microwave assisted extraction and high-performance liquid chromatography, *J. Pharm. Biomed. Anal.* 45 (3) (2007) 510–515.
- [20] X. Zhang, L. Xie, J. Long, Q. Xie, Y. Zheng, K. Liu, X. Li, Salidroside: a review of its recent advances in synthetic pathways and pharmacological properties, *Chem. Biol. Interact.* 339 (2021), 109268.
- [21] X. Zhang, Y. Zhang, R. Li, L. Zhu, B. Fu, T. Yan, Salidroside ameliorates Parkinson's disease by inhibiting NLRP3-dependent pyroptosis, *Aging (Albany NY)* 12 (10) (2020) 9405–9426.
- [22] Y. Cai, Y. Chai, Y. Fu, Y. Wang, Y. Zhang, X. Zhang, L. Zhu, M. Miao, T. Yan, Salidroside ameliorates alzheimer's disease by targeting NLRP3 inflammasome-mediated pyroptosis, *Front. Aging Neurosci.* 13 (2022), 809433.
- [23] S.S. Xing, J. Yang, W.J. Li, J. Li, L. Chen, Y.T. Yang, X. Lei, J. Li, K. Wang, X. Liu, Salidroside decreases atherosclerosis plaque formation via inhibiting endothelial cell pyroptosis, *Inflammation* 43 (2) (2020) 433–440.
- [24] J. Qian, X. Wang, W. Weng, G. Zhou, S. Zhu, C. Liu, Salidroside alleviates taurothiocholic acid 3-sulfate-induced AR42J cell injury, *Biomed. Pharmacother.* 142 (2021), 112062.
- [25] J. Qian, X.H. Wang, B.Z. Wei, G.X. Zhou, S.X. Zhu, C. Liu, Therapeutic effects of salidroside vs pyrrolidine dithiocarbamate against severe acute pancreatitis in rat, *J. Tradit. Chin. Med.* 42 (1) (2022) 49–57.
- [26] X. Wang, G. Zhou, C. Liu, R. Wei, S. Zhu, Y. Xu, M. Wu, Q. Miao, *Acanthopanax* versus 3-methyladenine ameliorates sodium taurocholate-induced severe acute pancreatitis by inhibiting the autophagic pathway in rats, *Mediat. Inflamm.* (2016), 8369704, 2016.
- [27] X. Wang, X. Zhuang, R. Wei, C. Wang, X. Xue, L. Mao, Protective effects of *Acanthopanax* vs. Ulinastatin against severe acute pancreatitis-induced brain injury in rats, *Int. Immunopharm.* 24 (2) (2015) 285–298.
- [28] X. Wang, L. Chu, C. Liu, R. Wei, X. Xue, Y. Xu, M. Wu, Q. Miao, Therapeutic effects of *Saussurea involucrata* injection against severe acute pancreatitis-induced brain injury in rats, *Biomed. Pharmacother.* 100 (2018) 564–574.
- [29] J. Schmidt, D.W. Rattner, K. Lewandrowski, C.C. Compton, U. Mandavilli, W.T. Knoefel, A.L. Warshaw, A better model of acute pancreatitis for evaluating therapy, *Ann. Surg.* 215 (1) (1992) 44–56.
- [30] D. Szklarczyk, A. Santos, C. von Mering, L.J. Jensen, P. Bork, M. Kuhn, *Stitch 5: augmenting protein-chemical interaction networks with tissue and affinity data*, *Nucleic Acids Res.* 44 (D1) (2016) D380–D384.
- [31] S. Jia, Y. Yang, Y. Bai, Y. Wei, H. Zhang, Y. Tian, J. Liu, L. Bai, Mechanical stimulation protects against chondrocyte pyroptosis through irisin-induced suppression of PI3K/Akt/NF- κ B signal pathway in osteoarthritis, *Front. Cell Dev. Biol.* 10 (2022), 797855.
- [32] S. Xu, J. Wang, J. Jiang, J. Song, W. Zhu, F. Zhang, M. Shao, H. Xu, X. Ma, F. Lyu, TLR4 promotes microglial pyroptosis via lncRNA-F630028O10Rik by activating PI3K/AKT pathway after spinal cord injury, *Cell Death Dis.* 11 (8) (2020) 693.
- [33] F. Shangquan, H. Zhou, N. Ma, S. Wu, H. Huang, G. Jin, S. Wu, W. Hong, W. Zhuang, H. Xia, L. Lan, A novel mechanism of cannabidiol in suppressing hepatocellular carcinoma by inducing GSDME dependent pyroptosis, *Front. Cell Dev. Biol.* 9 (2021), 697832.
- [34] M. Jiang, L. Qi, L. Li, Y. Li, The caspase-3/GSDME signal pathway as a switch between apoptosis and pyroptosis in cancer, *Cell Death Dis.* 6 (2020) 112.
- [35] P.J. Lee, G.I. Papachristou, New insights into acute pancreatitis, *Nat. Rev. Gastroenterol. Hepatol.* 16 (8) (2019 Aug) 479–496.
- [36] J. Wan, J. Chen, D. Wu, X. Yang, Y. Ouyang, Y. Zhu, L. Xia, N. Lu, Regulation of autophagy affects the prognosis of mice with severe acute pancreatitis, *Dig. Dis. Sci.* 63 (10) (2018) 2639–2650.
- [37] D. Ma, P. Jiang, Y. Jiang, H. Li, D. Zhang, Effects of lipid peroxidation-mediated ferroptosis on severe acute pancreatitis-induced intestinal barrier injury and bacterial translocation, *Oxid. Med. Cell. Longev.* 2021 (2021), 6644576.
- [38] J. Wu, J. Zhang, J. Zhao, S. Chen, T. Zhou, J. Xu, Treatment of severe acute pancreatitis and related lung injury by targeting gasdermin D-mediated pyroptosis, *Front. Cell Dev. Biol.* 9 (2021), 780142.
- [39] R. Kang, M.T. Lotze, H.J. Zeh, T.R. Billiar, D. Tang, Cell death and DAMPs in acute pancreatitis, *Mol. Med.* 20 (1) (2014) 466–477.
- [40] T. Lin, J. Song, X. Pan, Y. Wan, Z. Wu, S. Lv, L. Mi, Y. Wang, F. Tian, Downregulating gasdermin D reduces severe acute pancreatitis associated with pyroptosis, *Med. Sci. Mon. Int. Med. J. Exp. Clin. Res.* 27 (2021), e927968.
- [41] Q. Xu, M. Wang, H. Guo, H. Liu, G. Zhang, C. Xu, H. Chen, Emodin alleviates severe acute pancreatitis-associated acute lung injury by inhibiting the cold-inducible RNA-binding protein (CIRP)-mediated activation of the NLRP3/IL-1 β /CXCL1 signaling, *Front. Pharmacol.* 12 (2021), 655372.
- [42] J. Han, D. Chen, D. Liu, Y. Zhu, Modafinil attenuates inflammation via inhibiting Akt/NF- κ B pathway in apoE-deficient mouse model of atherosclerosis, *Inflammopharmacology* 26 (2) (2018) 385–393.
- [43] X. Han, B. Li, X. Ye, T. Mulatibieke, J. Wu, J. Dai, D. Wu, J. Ni, R. Zhang, J. Xue, R. Wan, X. Wang, G. Hu, Dopamine D2 receptor signalling controls inflammation in acute pancreatitis via a PP2A-dependent Akt/NF- κ B signalling pathway, *Br. J. Pharmacol.* 174 (24) (2017) 4751–4770.
- [44] M.J. Hossen, A. Amin, X.Q. Fu, J.Y. Chou, J.Y. Wu, X.Q. Wang, Y.J. Chen, Y. Wu, J. Li, C.L. Yin, C. Liang, G.X. Chou, Z.L. Yu, The anti-inflammatory effects of an ethanolic extract of the rhizome of *Atractylodes lancea*, involves Akt/NF- κ B signaling pathway inhibition, *J. Ethnopharmacol.* 277 (2021), 114183.
- [45] S. Xing, X. Yang, W. Li, F. Bian, D. Wu, J. Chi, G. Xu, Y. Zhang, S. Jin, Salidroside stimulates mitochondrial biogenesis and protects against H₂O₂-induced endothelial dysfunction, *Oxid. Med. Cell. Longev.* (2014), 904834, 2014.
- [46] Y. He, M. Ma, Y. Yan, C. Chen, H. Luo, W. Lei, Combined pre-conditioning with salidroside and hypoxia improves proliferation, migration and stress tolerance of adipose-derived stem cells, *J. Cell Mol. Med.* 24 (17) (2020) 9958–9971.
- [47] Y. Tang, Y. Hou, Y. Zeng, Y. Hu, Y. Zhang, X. Wang, X. Meng, Salidroside attenuates CoCl₂-simulated hypoxia injury in PC12 cells partly by mitochondrial protection, *Eur. J. Pharmacol.* 912 (2021), 174617.
- [48] H. Shang, S. Wang, J. Yao, C. Guo, J. Dong, L. Liao, Salidroside inhibits migration and invasion of poorly differentiated thyroid cancer cells, *Thorac. Canc.* 10 (6) (2019) 1469–1478.
- [49] N. Sayed, A. Khurana, C. Godugu, Pharmaceutical perspective on the translational hurdles of phytoconstituents and strategies to overcome, *J. Drug Deliv. Sci. Technol.* 53 (2019), 101201.